ACS APPLIED MATERIALS & INTERFACES

Research Article

www.acsami.org

$Mn^{II/III}$ Complexes as Promising Redox Mediators in Quantum-Dot-Sensitized Solar Cells

Andrew J. Haring, Michelle E. Pomatto, Miranda R. Thornton, and Amanda J. Morris*

Department of Chemistry, Virginia Tech, Blacksburg, Virginia 24061, United States

Supporting Information

ABSTRACT: The advancement of quantum dot sensitized solar cell (QDSSC) technology depends on optimizing directional charge transfer between light absorbing quantum dots, TiO_2, and a redox mediator. The nature of the redox mediator plays a pivotal role in determining the photocurrent and photovoltage from the solar cell. Kinetically, reduction of oxidized quantum dots by the redox mediator should be rapid and faster than the back electron transfer between TiO_2 and oxidized quantum dots to maintain photocurrent. Thermodynamically, the reduction potential of the redox mediator should be sufficiently positive to provide high photovoltages. To satisfy both criteria and enhance power conversion efficiencies, we introduced charge transfer spin-crossover $Mn^{II/III}$ complexes as promising redox mediator alternatives in QDSSCs. High photovoltages ~1 V were achieved by a series of Mn poly(pyrazolyl)borates, with reduction potentials ~0.51 V vs Ag/AgCl. Back electron transfer (recombination) rates were slower than $Co(bpy)_3$, where bpy = 2,2′-bipyridine, evidenced by electron lifetimes up to 4 orders of magnitude longer. This is indicative of a large barrier to electron transport imposed by spin-crossover in these complexes. Low solubility prevented the redox mediators from sustaining high photocurrent due to mass transport limits. However, with high fill factors (~0.6) and photovoltages, they demonstrate competitive efficiencies with $Co(bpy)_3$ redox mediator at the same concentration. More positive reduction potentials and slower recombination rates compared to current redox mediators establish the viability of Mn poly(pyrazolyl)borates as promising redox mediators. By capitalizing on these characteristics, efficient $Mn^{II/III}$-based QDSSCs can be achieved with more soluble Mn-complexes.

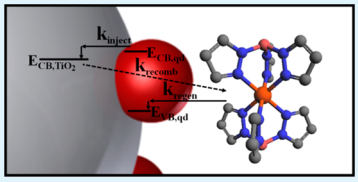

KEYWORDS: *quantum dot, solar cell, redox mediator, charge transfer-induced spin crossover, manganese*

INTRODUCTION

The 1985 discovery of fast photoelectron injection and slow recombination at TiO_2–Ru dye interfaces pioneered the modern field of light harvesting from sensitized TiO_2.[1] The observed long-lived charge separated state allowed Grätzel to capitalize on the efficient charge transfer by collecting the photoelectrons from TiO_2 as photocurrent with unprecedented efficiency.[2] By using mesoporous TiO_2 films with ~2000-fold higher surface area, O'Regan and Grätzel improved the dye adsorption yield and power conversion efficiency (7.1%) in dye-sensitized solar cells (DSSC).[3,4] As an alternative to molecular dye sensitizers, type II–VI semiconductor quantum dots (CdS and CdSe) exhibit fast photoelectron injection rates and have been employed in quantum dot-sensitized solar cells (QDSSC).[5−9] However, QDSSCs (record efficiencies ~7%) have yet to compete with that of DSSCs (13%) and remain the subject of continued research.[10−12]

In DSSCs, the iodide/triiodide couple serves to efficiently regenerate the ground state sensitizer, acting as a redox mediator to complete the electrical circuit between sensitized TiO_2 and the counter electrode. Much work has contributed to understanding the redox chemistry involved and the criteria necessary for optimization of the redox mediator, electrolyte additives, and solvent.[13−16] However, QDSSCs sensitized with cadmium chalcogenide quantum dots are unstable in the presence of iodide/triiodide due to photoanodic dissolution and the formation of cadmium iodide.[17] Therefore, sulfide/polysulfide electrolytes and suitable counter electrodes were developed to achieve stable QDSSCs.[18,19] Unfortunately, the unfavorably low redox potential, ~ 0.15 V vs Ag/AgCl, of the sulfide/polysulfide redox mediator system currently limits the performance of record liquid-junction QDSSCs. The resultant low photovoltages, ~0.6 V, have generated a need for the development of alternative redox mediators to improve photovoltages and overall efficiencies. To that end, metal complexes based on $Co^{II/III}$ centers, with tunable reduction potentials ~0.3–0.5 V vs Ag/AgCl, have garnered much attention as alternatives to the iodide/triiodide couple in DSSCs[20−25] but to a lesser extent in QDSSCs.[26−28]

The effectiveness of $Co^{II/III}$ mediators in DSSCs (>10%)[23] may be partly due to slow reduction kinetics of Co^{III} complexes, which undergo charge transfer-induced spin crossover transitions and internal reorganization upon electron transfer (d^6 to d^7).[22] Ideally, the oxidized redox mediator species M^{ox}, present at the TiO_2 surface, should not significantly reduce the lifetime of TiO_2 conduction band electrons ($TiO_2(e^-)s$) before M^{ox} diffuses to the counter electrode. The undesired recombination reaction between $TiO_2(e^-)s$ and M^{ox} limits charge collection, as with the ferrocene/ferrocenium couple, and constrains the choice of alternative mediators.[29] Some Mn^{III} complexes are

Received: May 20, 2014
Accepted: August 14, 2014
Published: August 19, 2014

 © 2014 American Chemical Society

known to undergo a spin change upon reduction (d^4 to d^5) that can slow the undesired recombination and have recently been employed in DSSCs.[30] Herein, the efficacy of $Mn^{II/III}$ complexes for use in QDSSCs is probed and shown to be an attractive alternative as redox mediators.

A series of Mn poly(pyrazolyl)borates, with reduction potentials more positive than $Co(bpy)_3$, where bpy =2,2′-bipyridine, and sulfide/polysulfide, delivered photovoltages ~1 V when coupled with CdS/CdSe cosensitized TiO_2 photoanodes. Photocurrents and incident-photon-to-current efficiency (IPCE) spectra similar to cells employing $Co(bpy)_3$ established the ability of the Mn^{II} complexes to regenerate ground state CdS and CdSe. Favorably, the Mn poly(pyrazolyl)borates display slower recombination at the TiO_2 photoanodes when compared to $Co(bpy)_3$, resulting in higher quasi-Fermi levels and, in turn, higher photovoltages. Thus, $Mn^{II/III}$ complexes are promising alternative redox mediators as they deliver efficiencies on average up to 50% higher than $Co(bpy)_3$. However, the low solubility of these complexes exacerbates mass transport limitations on redox mediators with slow diffusion properties and leads to limited photocurrents. Therefore, Mn poly(pyrazolyl)borates with higher solubility are the subject of continued research.

EXPERIMENTAL METHODS

Chemicals and Materials. Fluorine-doped tin oxide-coated glass (FTO-glass, 12−14 Ω cm^{-2}) from Hartford Glass Co., titanium(IV) chloride from Sigma-Aldrich, and Solaronix T/SP TiO_2 paste were used for photoanode preparation. Cadmium nitrate tetrahydrate (98%), cobalt chloride (98%), lithium perchlorate (99.99%), manganese chloride (97%), selenium dioxide (99.9%), sodium borohydride (98%), sodium sulfide (97%), and zinc acetate (99.99%) from Sigma-Aldrich were used without further purification. 2,2′-bipyridine (99%) was obtained from Acros Organics, nitrosium hexafluoroanimonate (97%) from Strem Chemicals, and sodium hexafluorophosphate (98%) from Oakwood Products. Ethanol from Decon Laboratories, methanol and acetone from Spectrum Chemical, and γ-butyrolactone from Sigma-Aldrich were used as solvents without further purification.

Synthesis of $Mn^{II/III}$ Complexes. $Mn^{II}(pzTp)_2$, $Mn^{II}(Tp)_2$, $Mn^{II}(Tp^*)_2$, where pzTp = tetrakis(pyrazolyl)borate, Tp = hydrotris(pyrazolyl)borate and Tp* = hydrotris(3,5-dimethylpyrazolyl)borate, and the oxidized salts $Mn^{III}(pzTp)_2SbF_6$, $Mn^{III}(Tp)_2SbF_6$ and $Mn^{III}(Tp^*)_2SbF_6$ were synthesized as previously described, (chemical structures in Figure S1 in the Supporting Information).[31] $MnCl_2$ was added to an aqueous solution of the respective poly(pyrazolyl)borate potassium salt (2 mol equiv., Strem Chemicals, 98%) and the Mn-poly(pyrazolyl)borate immediately precipitated. The Mn^{II} complexes were filtered, washed with copious amounts of water, and vacuum-dried. Oxidation of the complexes to Mn^{III} salts was achieved by addition of $NOSbF_6$ to the Mn^{II} complexes (1 mol equiv) in 1:1 acetonitrile/dichloroethane solutions and subsequent rotary evaporation and recrystallization from hot acetonitrile.

Synthesis of $Co^{II/III}$ Complexes. $Co^{II}(bpy)_3(PF_6)_2$ was synthesized as previously, where bpy =2,2′-bipyridine.[32] A methanolic solution of 2,2′-bipyridine (3.5 mmol) was added dropwise to an aqueous solution of $CoCl_2$ (2 mmol). With continued stirring, aqueous $NaPF_6$ (6.7 mmol) was added to precipitate the product. The precipitate was then filtered, dried, recrystallized from hot ethyl acetate, and dried under vacuum to obtain $Co^{II}(bpy)_3(PF_6)_2$.

$Co^{III}(bpy)_3(PF_6)_3$ was synthesized by chemically oxidizing $Co^{II}(bpy)_3^{2+}$ before adding $NaPF_6$. A solution of 2,2′-bipyridine and $CoCl_2$ was prepared as above. Concentrated HCl and 30% H_2O_2 were added simultaneously to the stirring mixture (2 mL each).[23] The solution was heated at 50 °C for 45 min, during which time a burnt orange color developed. Aqueous $NaPF_6$ (6.7 mmol) was added to precipitate the product. The precipitate was then filtered, dried, recrystallized from hot ethyl acetate, and dried under vacuum to obtain $Co^{III}(bpy)_3(PF_6)_3$.

Device Fabrication. *Photoanode Preparation.* FTO-glass was ultrasonicated for 15 min in aqueous Alconox detergent and rinsed with deionized water. The sonication/rinsing cycle was repeated with ethanol and acetone, respectively. A compact TiO_2 layer was deposited by heating FTO-glass in 40 mM $TiCl_{4(aq)}$ for 30 min before doctor-blading Solaronix T/SP paste (100% anatase, 15−20 nm). The TiO_2 films were heated at 80 °C for 30 min before a 7°/min ramp to 450 °C and held at 450 °C for 30 min.

Successive Ionic Layer Adsorption and Reaction (SILAR). A SILAR method was used to sequentially deposit CdS, CdSe, and ZnS onto the mesoporous TiO_2 films.[27] Each SILAR cycle consists of soaking the annealed TiO_2 films in cationic solutions (Cd^{2+} or Zn^{2+}) for 1 min, rinsing with the respective neat solvent, soaking in anionic solutions (S^{2-} or Se^{2-}) for 1 min, and rinsing again with neat solvent. Thus, all TiO_2 photoanodes are coated first, with CdS quantum dots, second, with a layer of CdSe, and last, with a passivation layer of ZnS, as verified by absorption spectroscopy, Figure S2 in the Supporting Information.[33,34] For CdS SILAR deposition, 0.1 M $Cd(NO_3)_2$ and 0.1 M Na_2S solutions were used (1:1 methanol/water, 6 cycles). For CdSe SILAR deposition, 0.03 M cadmium nitrate and 0.03 M selenium dioxide solutions were used (ethanol, 8 cycles). Solutions of Se^{2-} were prepared from selenium dioxide by adding 2 equiv. of $NaBH_4$ and stirring under nitrogen atmosphere until clear. For ZnS SILAR deposition, 0.1 M $Zn(CH_3COOH)_2$ and 0.1 M Na_2S solutions were used (1:1 methanol/water, 2 cycles).

Electrochemistry. Cyclic voltammetry and potential-step chronoamperometry of Mn^{II} complexes were performed in γ-butyrolactone with 0.1 M $LiClO_4$ supporting electrolyte with a Pt mesh counter, a Pt or glassy carbon working, and an Ag/AgCl saturated KCl reference electrode, calibrated with $K_4[Fe(CN)_6]$ from Fisher Scientific. Potentials were applied with a BASi Epsilon potentiostat (0.01−10 V/s). For potential-step chronoamperometry, potentials were applied sufficiently reductive so that the current measured was diffusion limited.

Photovoltaic Characterization. The Mn-complexes were tested and compared to $Co(bpy)_3$ as redox mediators in conjunction with the photoanodes fabricated above. A three-electrode arrangement was employed with the quantum dot-sensitized photoanode as the working electrode, a Pt mesh counter electrode, and an Ag/AgCl reference electrode. The electrolyte (0.35 mL) consisted of 0.1 M $LiClO_4$, 50 mM M^{II}, and 5 mM M^{III} in γ-butyrolactone, where M^{II} and M^{III} represent the reduced and oxidized form of the respective redox mediator complex. Among common liquid-junction solar cell solvents, the Mn-complexes were most soluble in γ-butyrolactone.[35] A masked area of 0.1256 cm^2 was illuminated at various intensities with a Newport LCS-100 solar simulator (AM 1.5G spectrum) and current−voltage responses were recorded at a scan rate of 25 mV/s. Incident-photon-to-current efficiency (IPCE) spectra were collected at short-circuit conditions using a monochromatized light source from Optical Building Blocks (OBB). Open circuit voltage decay measurements were collected by interrupting the illumination and monitoring the voltage decay at 50 ms data intervals.[36]

RESULTS AND DISCUSSION

The operation of sensitized solar cells depends on directional and regenerative photoelectrochemical charge transfer upon illumination in order to convert incident photons to photocurrent. Therefore, in QDSSCs efficient generation of photocurrent is mediated by (1) fast electron injection from photoexcited QDs to TiO_2, (2) fast reduction of the oxidized QDs by reduced redox mediator species, and 3) slow charge recombination between $TiO_2(e^-)$s and the M^{ox} species (eq 1), Figure 1. Within the $TiO_2(e^-)$ lifetime, τ_e, photoelectrons must be transported through the mesoporous film and collected at the FTO−glass substrate.

$$TiO_2(e^-) + M^{ox} \rightarrow TiO_2 + M^{red} \quad (1)$$

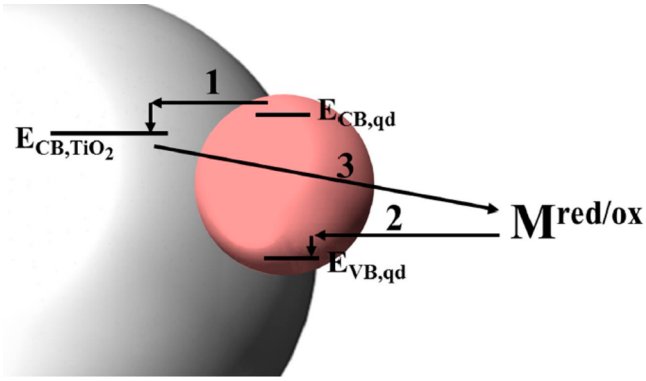

Figure 1. Energy schematic of electron transfer at the quantum dot-TiO_2 interface: (1) photoelectron injection from the quantum dot conduction band ($E_{CB,qd}$) into the TiO_2 conduction band ($E_{CB,TiO2}$), (2) reduction of the quantum dot into the valence band ($E_{VB,qd}$) by reduced mediator species, (3) undesired recombination of $TiO_2(e^-)$s with oxidized mediator species.

Thus, a series of Mn-complexes, $Mn^{II}(pzTp)_2$, $Mn^{II}(Tp)_2$, and $Mn^{II}(Tp^*)_2$, with slow reduction kinetics were chosen to avoid shortening τ_e by the charge transfer from $TiO_2(e^-)$s to Mn^{III}. The one-electron reduction of Mn^{III}poly(pyrazolyl)-borates results in a low spin to high spin transition ($t_{2g}^4 \rightarrow t_{2g}^3e_g^2$; $S = 1 \rightarrow 5/2$).[31] Becaues of this charge-transfer-induced spin crossover, the standard electrochemical rate constants are slow ($Fc^{0/+}$ (1×10^0 cm/s) > $Co^{II/III}$ (1×10^{-1} cm/s) > $Mn^{II/III}$ (1×10^{-4}) cm/s)) and decrease in the ligand series Tp* > pzTp > Tp.[31,37,38] At the TiO_2 anode surface, an additional thermodynamic barrier is imposed by the spin transition and reorganization energy associated with the transition, which should slow recombination (process 3 in Figure 1).

Additionally, maximization of the photocurrent generated from illumination of QDs requires minimization of competitive light absorption by other solar cell components, including the redox mediator. Therefore, the ideal species should absorb minimally in the absorption range of CdS/CdSe quantum dots (700−400 nm). Compared to sulfide redox mediator, manganese poly(pyrazolyl)borates display less absorption in the desired range, Figure 2. Mn^{II} species have no appreciable absorbance above ∼420 nm (<3 M^{-1} cm^{-1}), see Figure S3 in the Supporting Information. The absorbance of Mn^{III} species extends further into the visible region, with absorbance at ∼440 nm (∼184 M^{-1} cm^{-1}), although with a lower extinction coefficient than Na_2S/S at similar wavelengths (∼277 M^{-1} cm^{-1}).

To determine the viability of Mn-complexes as redox mediators in QDSSCs, we analyzed the light-harvesting performance of the photoanode/electrolyte combination by fabricating and testing three-electrode cells. In three electrode arrangements, as opposed to complete solar cells, the performance of the photoanode/electrolyte combination is isolated from counter electrode effects (mass transport and charge transfer overpotentials). Therefore, the charge-transfer kinetics and energetics at the photoanode can be studied and optimized independently of the counter electrode kinetics. However, the spin-crossover barrier that slows recombination must be overcome by the counter electrode. As the subject of continued research, counter electrodes will be designed to

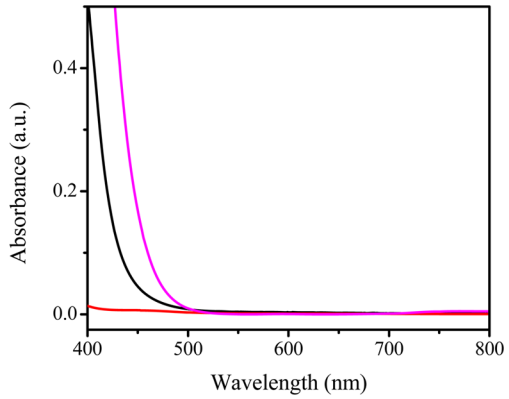

Figure 2. Visible absorbance spectra of redox mediators used in QDSSCs. Black, 1 mM of $Mn(Tp)_2$, 0.1 mM $Mn(Tp)_2SbF_6$; red, 1 mM $Co(bpy)_3(PF_6)_2$, 0.1 mM $Co(bpy)_3(PF_6)_3$; and magenta, 1 mM Na_2S, 1 mM S. A baseline of the respective solvents was subtracted.

sufficiently catalyze the reduction of Mn^{III} species, minimizing charge-transfer overpotentials that would reduce power conversion efficiencies. CdS/CdSe-sensitized TiO_2 served as the photoanode in contact with the respective electrolyte. Cells containing Mn-complexes were compared to $Co(bpy)_3$. Sulfide/polysulfide was not compared because of its lack of chemical stability in γ-butyrolactone.

Current density−voltage ($J-V$) plots with QD-sensitized TiO_2 photoanodes and electrolytes with the Mn-complexes are shown with different illumination intensities in Figure 3. Figures of merit for 20% and 100% sun intensity are tabulated in Table 1 and Table S1 in the Supporting Information, respectively; data from individual trials are tabulated in Table S2 in the Supporting Information. Overall efficiency averages, η, trend as $Mn(Tp^*)_2 \sim Co(bpy)_3 < Mn(pzTp)_2 < Mn(Tp)_2$. For $Mn(Tp)_2$, increases in photovoltage and fill factor lead to efficiencies competitive with the known redox mediator, $Co(bpy)_3$, and the best performing cells were twice as efficient. Comparison of $J-V$ curves for Mn-complexes and $Co(bpy)_3$ are shown in Figure S5 in the Supporting Information. Further insight into solar cell performance is gained by analyzing the trends in photovoltages, fill factor, and photocurrent, which compose overall efficiencies.

To maximize the photovoltage, ideal redox mediators should have sufficiently positive reduction potentials (>0.1 vs Ag/AgCl). In QDSSCs, the theoretical upper limit photovoltage is determined by the potential difference between the electron Fermi level in TiO_2 under illumination ($E_{F,n}$) and the redox potential of the redox mediator.[39,40] Photovoltages approaching the upper limit can be obtained by employing redox mediators with reduction potentials >0.15 V vs Ag/AgCl while still maintaining sufficient reductive power to reduce QDs, process 2 in Figure 1. Cyclic voltammetry shows $E_{1/2}$ values of ∼0.51 V vs Ag/AgCl for the series of Mn poly(pyrazolyl)borates studied, Figure 4, which is 0.4 V more positive than Na_2S/S and 0.1−0.2 V more positive than typical $Co^{II/III}$ complexes.[22] With such positive reduction potentials, the Mn-complexes still demonstrated sufficient driving force to reduce photooxidized QDs and act as viable alternative redox mediators. The high V_{oc} values ∼1 V (x-axis intercept, Figure 3) are consistent with the positive reduction potentials discussed above, as the photovoltages increase with reduction potential, $Co(bpy)_3 < Mn(Tp)_2 \sim Mn(Tp^*)_2 < Mn(pzTp)_2$.

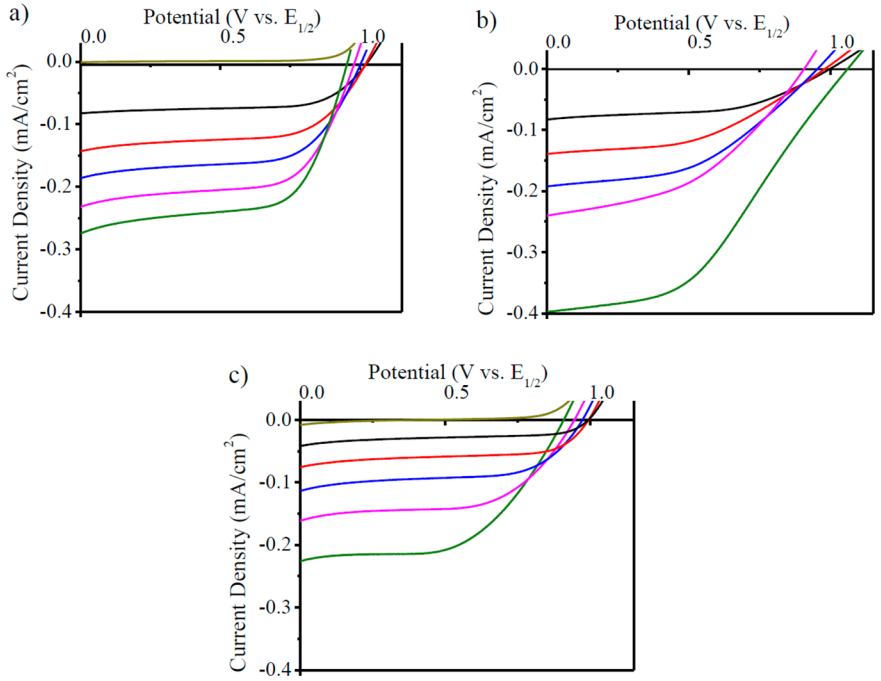

Figure 3. $J-V$ plots of three-electrode arrangement with (a) 50 mM $Mn(pzTp)_2$ and 5 mM $Mn(pzTp)_2SbF_6$, (b) 50 mM $Mn(Tp)_2$ and 5 mM $Mn(Tp)_2SbF_6$, and (c) 50 mM $Mn(Tp^*)_2$ and 5 mM $Mn(Tp^*)_2SbF_6$. All electrolytes contain 0.1 M $LiClO_4$ in γ-butyrolactone. Potentials scanned from reverse to forward bias at 25 mV/s. Dark yellow, dark current; black, 20% sun; red, 40% sun; blue, 60% sun; magenta, 80% sun; green, 100% sun (100 mW/cm^2).

Table 1. Figures of Merit for Cells Containing Mn or Co Complexes at 20% Sun Intensity

	J_{sc} (mA/cm^2)	V_{oc} (V)	fill factor	η (%)	$E_{1/2}$ (V vs Ag/AgCl)
$Mn(pzTp)_2$	−0.08 ± 0.02	1.08 ± 0.06	0.66 ± 0.2	0.24 ± 0.04	0.52
$Mn(Tp)_2$	−0.12 ± 0.02	0.9 ± 0.1	0.55 ± 0.1	0.33 ± 0.15	0.51
$Mn(Tp^*)_2$	−0.06 ± 0.02	1.01 ± 0.02	0.58 ± 0.08	0.19 ± 0.09	0.51
$Co(bpy)_3$	−0.12 ± 0.02	0.8 ± 0.1	0.45 ± 0.09	0.22 ± 0.04	0.36[32]

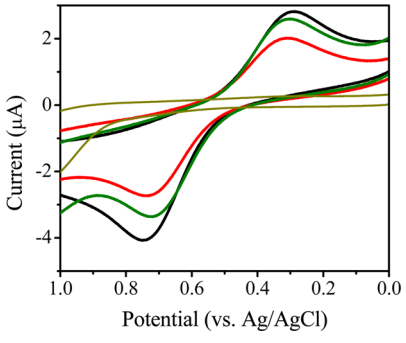

Figure 4. Cyclic voltammograms of $Mn(pzTp)_2$ (black), $Mn(Tp)_2$ (red), $Mn(Tp^*)_2$ (green), and supporting electrolyte only (dark yellow): γ-butyrolactone with 0.1 M $LiClO_4$ with a Pt working electrode. $E_{1/2}$ values are tabulated in Table 1

Both fill factor and photovoltage are influenced by recombination kinetics. Long τ_e increase the concentration of $TiO_2(e^-)$s and, thus, $E_{F,n}$ contributing to a higher V_{oc}. High fill factor depends on recombination kinetics by the ability to sustain photocurrent under applied bias. At applied potentials near V_{oc}, the reduction of Mn^{III} species by $TiO_2(e^-)$s is slow, eq 1, maintaining long τ_e. τ_e is measured by monitoring the open circuit voltage decay (OCVD) from illumination conditions to equilibrium dark conditions.[36,40] The time derivative of the voltage decay, scaled by the thermal voltage, is used to extract τ_e.[41]

$$\tau_e = -\frac{k_B T}{e}\left(\frac{dV_{oc}}{dt}\right)^{-1} \quad (2)$$

From plots of τ_e vs V_{oc}, recombination kinetics can be qualitatively compared between cells of different redox mediators, Figure 5. Lifetimes at a given voltage increase in

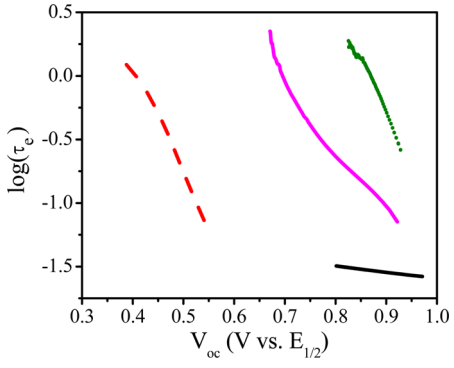

Figure 5. Electron lifetimes extracted from open circuit voltage decay measurements (OCVD) by eq S2 in the Supporting Information. $Mn(Tp)_2$ (solid magenta), $Mn(pzTp)_2$ (dotted green), $Mn(Tp^*)_2$ (solid black), and $Co(bpy)_3$ (dashed red).

dx.doi.org/10.1021/am503138d | ACS Appl. Mater. Interfaces 2014, 6, 15061−15067

the order $Mn(Tp^*)_2$ < $Mn(Tp)_2$ < $Mn(pzTp)_2$. Consistent with the longest lifetimes, cells employing $Mn(pzTp)_2$ demonstrate the highest fill factors and photovoltages. By extrapolating $Co(bpy)_3$ data to higher voltages, the Mn-complexes demonstrate lifetimes 2−4 orders of magnitude longer than $Co(bpy)_3$ at the same V_{oc}. For $Mn^{II/III}$, the slower undesired recombination reaction is likely due to the effective charge transfer-induced spin crossover, further supporting the viability of Mn poly(pyrazolyl)borates as alternative redox mediators. Although both $Co(bpy)_3$ and the Mn-complexes undergo charge transfer-induced spin crossover upon reduction (d^6 to d^7 for Co and d^4 to d^5 for Mn), the barrier toward reduction is larger for the Mn-complexes. Structural and electronic differences between the Co- and Mn-complexes will affect the reduction barrier through reorganization energies, electron pairing energies, and ligand field splitting.

The low solubility of the Mn-complexes studied (50 mM in γ-butyrolactone) drastically limits the photocurrent, which is typically 1−3 mA/cm^2 in 0.1−0.3 M Co-based QDSSCs and 10−20 mA/cm^2 in 1−2 M sulfide-based QDSSCs.[18,26,33,42] This is not surprising given that even at typical concentrations used in DSSCs (0.1−0.3 M) Co polypyridyl complexes experience mass transport limitations not seen with the smaller iodide/triiodide or sulfide/polysulfide redox couples.[43,44] The effect of mass transport observed for the Mn-complexes at low concentrations is further complicated by an additional diffusive kinetic barrier, corresponding to interstitial Mn^{III} within the sensitized TiO_2. For direct comparison, tests with $Co(bpy)_3$ redox mediator were intentionally kept at the same concentration as the Mn-complexes.

Low photocurrent compared to optimized QDSSCs (1−3 mA/cm^2), obtained with all redox mediators, tested does not diminish the promising effectiveness of $Mn^{II/III}$ complexes. Rather, the primary contributions to the observed diffusion-limited photocurrents are likely the unoptimized porosity of the QD-sensitized TiO_2 films and the relatively long distance between the TiO_2 film and counter electrode in the experimental setup (8 mm). High photocurrents form concentration gradients of M^{red} and M^{ox} between the TiO_2 film and counter electrode that require initial concentrations of M^{red} ≫50 mM. From Fick's first law of diffusion, the concentration gradient can be related to photocurrent (dependent on one electron transfer with redox species), assuming a linear concentration gradient, eq 3

$$D_o \frac{dC_o}{dx} = \frac{j}{F} \tag{3}$$

where D_o, the diffusion coefficient of redox mediator species, is assumed to be constant throughout the TiO_2 film and bulk solution for simplicity, F is Faraday's constant, and j is the photocurrent density. Diffusion coefficients of Mn-complexes in γ-butyrolactone were determined by potential-step Cottrell analysis shown in the Supporting Information, Figure S4. For QDSSC three electrode cells with $Mn^{II}(Tp)_2$ (D_o = 2 × 10^{-5} cm^2/s) producing j = 0.12 mA/cm^2, a concentration gradient of 60 mM/cm^2 forms between the electrodes (dC_o ≈ 50 mM). Therefore, considering an initial concentration of 50 mM, $Mn^{II}(Tp)_2$ is depleted at the photoanode under 20% sun illumination (20 mW/cm^2). The photocurrent is limited by diffusion rather than the ability of $Mn^{II}(Tp)_2$ to reduce oxidized CdS/CdSe quantum dots. Similarly, smaller values of D_o for $Mn(Tp^*)_2$ and $Mn(pzTp)_2$ (1 × 10^{-5} cm^2/s and 0.6 × 10^{-5} cm^2/s, respectively) supported lower photocurrents before being depleted at the photoanode.

Incident-photon-to-current efficiency (IPCE) spectra provide a greater understanding of the observed low photocurrents, Figure 6. The IPCE is the product of the light harvesting (α),

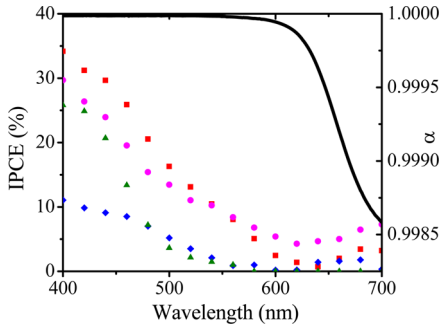

Figure 6. Left y-axis: Incident-photon-to-current efficiency (IPCE) spectra of three-electrode arrangement with $Mn(pzTp)_2$ (green triangles), $Mn(Tp)_2$ (magenta circles), $Mn(Tp^*)_2$ (blue diamonds), and $Co(bpy)_3$ (red squares) redox mediator (∼1 mW/cm^2 illumination). Right y-axis: Light harvesting efficiency (α) of quantum dot-sensitized TiO_2 based on absorbance spectrum of sensitized films.

charge injection (η_{in}) and charge collection (η_{cc}) efficiencies according to eq 4

$$\text{IPCE} = \alpha\eta_{in}\eta_{cc} \tag{4}$$

Opaque black photoanodes of CdS/CdSe-TiO_2 absorb in the visible region, minimizing the effect of α, Figure 6. If α is the limiting factor, then IPCE ≅ α and the IPCE and absorbance spectra should coincide, which is not observed. Therefore, the reduced IPCE is likely due to inefficient charge injection or charge collection, which explains the difference in profile between IPCE and α. It is reasonable to assume that charge collection is the limiting factor since it depends on the reduction of oxidized CdS/CdSe quantum dots by M^{red} species, which would be depleted at the quantum dot surface as described above (diffusion limited photocurrents). .

Additionally, the trend in photocurrents among the Mn-complex ligand series is consistent with the trend in standard electrochemical rate constants, mentioned above. The electrochemical rate constant for M^{ox} to M^{red} charge transfer affects the undesired recombination reaction kinetics, eq 1. As the electrochemical rate constants of the redox mediators decrease, the initial J_{sc} values increase because of slower recombination processes, Tp* < pzTp < Tp. At steady-state conditions, however, the concentration gradient of the M^{red} species imposes mass transport limits to the observed photocurrents.

CONCLUSIONS

To improve the efficiency of QDSSCs, new redox mediators need to be developed that display positive reduction potentials and slow charge recombination rates. Therefore, Mn poly(pyrazolyl)borate have been demonstrated as viable alternatives. The charge transfer-induced spin crossover transition, upon regenerative oxidation by photoexcited quantum dots, reduces the undesired recombination reaction at the TiO_2 surface. Slow recombination kinetics near operating voltages led to high fill factors and contributed to high $E_{F,n}$. Thus, coupled to positive reduction potentials, impressive photovoltages ∼1 V result. To realize photocurrent densities in the

mA/cm^2 range, limitations imposed by mass transport can be alleviated by designing Mn poly(pyrazolyl)borates with higher solubilities in typical QDSSC electrolyte solvents and is the subject of continued research.

■ ASSOCIATED CONTENT

Supporting Information

Chemical structures of the Mn complexes, Cottrell analysis for diffusion coefficients, and $J-V$ figures of merit for 100% sun intensity (100 mW/cm^2). This material is available free of charge via the Internet at http://pubs.acs.org/.

■ AUTHOR INFORMATION

Corresponding Author

*E-mail: ajmorris@vt.edu.

Notes

The authors declare no competing financial interest.

■ ACKNOWLEDGMENTS

The authors are grateful for funding provided by the Institute for Critical Technology and Applied Science, Oak Ridge Associated Universities, and the Chemistry Department at Virginia Tech. The authors thank the College of Science at Virginia Tech for funding the Solar Testing Center.

■ REFERENCES

(1) De Silvestro, J.; Gratzel, M.; Kavan, L.; Moser, J.; Augustynski, J. Highly Efficient Sensitization of Titanium-Dioxide. *J. Am. Chem. Soc.* **1985**, *107*, 2988−2990.

(2) Vlachopoulos, N.; Liska, P.; Augustynski, J.; Gratzel, M. Very Efficient Visible-Light Energy Harvesting and Conversion by Spectral Sensitization of High Surface-Area Polycrystalline Titanium-Dioxide Films. *J. Am. Chem. Soc.* **1988**, *110*, 1216−1220.

(3) O'Regan, B.; Gratzel, M. A Low-Cost, High-Efficiency Solar-Cell Based on Dye-Sensitized Colloidal TiO_2 Films. *Nature* **1991**, *353*, 737−740.

(4) Hagfeldt, A.; Boschloo, G.; Sun, L. C.; Kloo, L.; Pettersson, H. Dye-Sensitized Solar Cells. *Chem. Rev.* **2010**, *110*, 6595−6663.

(5) Tvrdy, K.; Frantsuzov, P. A.; Kamat, P. V. Photoinduced Electron Transfer from Semiconductor Quantum Dots to Metal Oxide Nanoparticles. *Proc. Natl. Acad. Sci. U.S.A.* **2011**, *108*, 29−34.

(6) Robel, I.; Kuno, M.; Kamat, P. V. Size-Dependent Electron Injection from Excited CdSe Quantum Dots into TiO_2 Nanoparticles. *J. Am. Chem. Soc.* **2007**, *129*, 4136−4137.

(7) Gopidas, K. R.; Bohorquez, M.; Kamat, P. V. Photoelectrochemistry in Semiconductor Particulate Systems. 16. Photophysical and Photochemical Aspects of Coupled Semiconductors - Charge-Transfer Processes in Colloidal CdS-TiO_2 and CdS-AgI Systems. *Pharm. Pharmacol. Lett.* **1990**, *94*, 6435−6440.

(8) Yu, W. W.; Qu, L. H.; Guo, W. Z.; Peng, X. G. Experimental Determination of the Extinction Coefficient of CdTe, CdSe, and CdS Nanocrystals. *Chem. Mater.* **2003**, *15*, 2854−2860.

(9) Yu, W. W.; Qu, L. H.; Guo, W. Z.; Peng, X. G. Experimental Determination of the Extinction Coefficient of CdTe, CdSe and Cds Nanocrystals. *Chem. Mater.* **2004**, *16*, 560−560.

(10) Yella, A.; Lee, H. W.; Tsao, H. N.; Yi, C. Y.; Chandiran, A. K.; Nazeeruddin, M. K.; Diau, E. W. G.; Yeh, C. Y.; Zakeeruddin, S. M.; Gratzel, M. Porphyrin-Sensitized Solar Cells with Cobalt$^{(II/III)}$-Based Redox Electrolyte Exceed 12% Efficiency. *Science* **2011**, *334*, 629−634.

(11) Mathew, S.; Yella, A.; Gao, P.; Humphry-Baker, R.; Curchod, B. F. E.; Ashari-Astani, N.; Tavernelli, I.; Rothlisberger, U.; Nazeeruddin, M. K.; Gratzel, M. Dye-Sensitized Solar Cells with 13% Efficiency Achieved Through the Molecular Engineering of Porphyrin Sensitizers. *Nat. Chem.* **2014**, *6*, 242−247.

(12) Wang, J.; Mora-Sero, I.; Pan, Z. X.; Zhao, K.; Zhang, H.; Feng, Y. Y.; Yang, G.; Zhong, X. H.; Bisquert, J. Core/Shell Colloidal Quantum Dot Exciplex States for the Development of Highly Efficient Quantum-Dot-Sensitized Solar Cells. *J. Am. Chem. Soc.* **2013**, *135*, 15913−15922.

(13) Fisher, A. C.; Peter, L. M.; Ponomarev, E. A.; Walker, A. B.; Wijayantha, K. G. U. Intensity Dependence of the Back Reaction and Transport of Electrons in Dye-Sensitized Nanocrystalline TiO_2 Solar Cells. *J. Phys. Chem. B* **2000**, *104*, 949−958.

(14) Huang, S. Y.; Schlichthorl, G.; Nozik, A. J.; Gratzel, M.; Frank, A. J. Charge Recombination in Dye-Sensitized Nanocrystalline TiO_2 Solar Cells. *J. Phys. Chem.B* **1997**, *101*, 2576−2582.

(15) Gardner, J. M.; Giaimuccio, J. M.; Meyer, G. J. Evidence for Iodine Atoms as Intermediates in the Dye Sensitized Formation of I-I Bonds. *J. Am. Chem. Soc.* **2008**, *130*, 17252−17253.

(16) Nazeeruddin, M. K.; Kay, A.; Rodicio, I.; Humphrybaker, R.; Muller, E.; Liska, P.; Vlachopoulos, N.; Gratzel, M. Conversion of Light to Electricity by *cis*-X_2Bis(2,2′-Bipyridyl-4,4′-Dicarboxylate)-Ruthenium(II) Charge-Transfer Sensitizers (X = Cl^-, Br^-, I^-, CN^-, and SCN^-) on Nanocrystalline TiO_2 Electrodes. *J. Am. Chem. Soc.* **1993**, *115*, 6382−6390.

(17) Nakatani, K.; Matsudaira, S.; Tsubomura, H. Photoanodic Behavior of n-type Cadmium-Sulfide in Acetonitrile Solutions Containing Iodide-Ion. *J. Electrochem. Soc.* **1978**, *125*, 406−409.

(18) Radich, J. G.; Dwyer, R.; Kamat, P. V. Cu_2S Reduced Graphene Oxide Composite for High-Efficiency Quantum Dot Solar Cells. Overcoming the Redox Limitations of S_2^-/S_n^{2-} at the Counter Electrode. *J. Phys. Chem. Lett.* **2011**, *2*, 2453−2460.

(19) Kamat, P. V.; Christians, J. A.; Radich, J. G. Quantum Dot Solar Cells: Hole Transfer as a Limiting Factor in Boosting the Photoconversion Efficiency. *Langmuir* **2014**, DOI: 10.1021/la500555w.

(20) Nusbaumer, H.; Moser, J. E.; Zakeeruddin, S. M.; Nazeeruddin, M. K.; Gratzel, M. Co-II(dbbip)$_2^{2+}$ Complex Rivals Tri-Iodide/Iodide Redox Mediator in Dye-Sensitized Photovoltaic Cells. *J. Phys. Chem. B* **2001**, *105*, 10461−10464.

(21) Sapp, S. A.; Elliott, C. M.; Contado, C.; Caramori, S.; Bignozzi, C. A. Substituted Polypyridine Complexes of Cobalt$^{(II/III)}$ as Efficient Electron-Transfer Mediators in Dye-Sensitized Solar Cells. *J. Am. Chem. Soc.* **2002**, *124*, 11215−11222.

(22) Nusbaumer, H.; Zakeeruddin, S. M.; Moser, J. E.; Gratzel, M. An Alternative Efficient Redox Couple for the Dye-Sensitized Solar Cell System. *Chem.—Eur. J.* **2003**, *9*, 3756−3763.

(23) Yum, J. H.; Baranoff, E.; Kessler, F.; Moehl, T.; Ahmad, S.; Bessho, T.; Marchioro, A.; Ghadiri, E.; Moser, J. E.; Yi, C. Y.; Nazeeruddin, M. K.; Gratzel, M. A Cobalt Complex Redox Shuttle for Dye-Sensitized Solar Cells with High Open-Circuit Potentials. *Nat. Commun.* **2012**, *3*, 631.

(24) Feldt, S. M.; Wang, G.; Boschloo, G.; Hagfeldt, A. Effects of Driving Forces for Recombination and Regeneration on the Photovoltaic Performance of Dye-Sensitized Solar Cells using Cobalt Polypyridine Redox Couples. *J. Phys. Chem. C* **2011**, *115*, 21500−21507.

(25) Achari, M. B.; Elumalai, V.; Vlachopoulos, N.; Safdari, M.; Gao, J. J.; Gardner, J. M.; Kloo, L. A Quasi-Liquid Polymer-Based Cobalt Redox Mediator Electrolyte for Dye-Sensitized Solar Cells. *Phys. Chem. Chem. Phys.* **2013**, *15*, 17419−17425.

(26) Lee, H. J.; Yum, J. H.; Leventis, H. C.; Zakeeruddin, S. M.; Haque, S. A.; Chen, P.; Seok, S. I.; Grazel, M.; Nazeeruddin, M. K. CdSe Quantum Dot-Sensitized Solar Cells Exceeding Efficiency 1% at Full-Sun Intensity. *J. Phys. Chem. C* **2008**, *112*, 11600−11608.

(27) Lee, H.; Wang, M. K.; Chen, P.; Gamelin, D. R.; Zakeeruddin, S. M.; Gratzel, M.; Nazeeruddin, M. K. Efficient CdSe Quantum Dot-Sensitized Solar Cells Prepared by an Improved Successive Ionic Layer Adsorption and Reaction Process. *Nano Lett.* **2009**, *9*, 4221−4227.

(28) Lee, H. J.; Chen, P.; Moon, S. J.; Sauvage, F.; Sivula, K.; Bessho, T.; Gamelin, D. R.; Comte, P.; Zakeeruddin, S. M.; Il Seok, S.; Gratzel, M.; Nazeeruddin, M. K. Regenerative PbS and CdS Quantum Dot Sensitized Solar Cells with a Cobalt Complex as Hole Mediator. *Langmuir* **2009**, *25*, 7602−7608.

(29) Gregg, B. A.; Pichot, F.; Ferrere, S.; Fields, C. L. Interfacial Recombination Processes in Dye-Sensitized Solar Cells and Methods to Passivate the Interfaces. *J. Phys. Chem. B* **2001**, *105*, 1422−1429.
(30) Perera, I. R.; Gupta, A.; Xiang, W.; Daeneke, T.; Bach, U.; Evans, R. A.; Ohlin, C. A.; Spiccia, L. Introducing Manganese Complexes as Redox Mediators for Dye-Sensitized Solar Cells. *Phys. Chem. Chem. Phys.* **2014**, DOI: 10.1039/C3CP54894E.
(31) Hossain, F.; Rigsby, M. A.; Duncan, C. T.; Milligan, P. L.; Lord, R. L.; Baik, M. H.; Schultz, F. A. Synthesis, structure, and properties of low-spin manganese(III)-poly(pyrazolyl)borate complexes. *Inorg. Chem.* **2007**, *46*, 2596−2603.
(32) Liu, Y. R.; Jennings, J. R.; Huang, Y.; Wang, Q.; Zakeeruddin, S. M.; Gratzel, M. Cobalt Redox Mediators for Ruthenium-Based Dye-Sensitized Solar Cells: A Combined Impedance Spectroscopy and Near-IR Transmittance Study. *J. Phys. Chem. C* **2011**, *115*, 18847−18855.
(33) Santra, P. K.; Kamat, P. V. Mn-Doped Quantum Dot Sensitized Solar Cells: A Strategy to Boost Efficiency over 5%. *J. Am. Chem. Soc.* **2012**, *134*, 2508−2511.
(34) Yu, X. Y.; Lei, B. X.; Kuang, D. B.; Su, C. Y. High performance and reduced charge recombination of CdSe/CdS quantum dot-sensitized solar cells. *J. Mater. Chem.* **2012**, *22*, 12058−12063.
(35) Hagfeldt, A.; Boschloo, G.; Sun, L. C.; Kloo, L.; Pettersson, H. Dye-Sensitized Solar Cells. *Chem. Rev.* **2010**, *110*, 6595−6663.
(36) Zaban, A.; Greenshtein, M.; Bisquert, J. Determination of the Electron Lifetime in Nanocrystalline Dye Solar Cells by Open-Circuit Voltage Decay Measurements. *ChemPhysChem.* **2003**, *4*, 859−864.
(37) Fu, Y. S.; Cole, A. S.; Swaddle, T. W. Solvent Dynamics and Pressure Effects in the Kinetics of the Tris(Bipyridine)Cobalt(III/II) Electrode Reaction in Various Solvents. *J. Am. Chem. Soc.* **1999**, *121*, 10410−10415.
(38) Ito, N.; Saji, T.; Aoyagui, S. Electrochemical Formation of Stable Ferrocene Ion and the Formal Rate-Constant of the Ferrocene$^{0/-}$ Electrode. *J. Organomet. Chem.* **1983**, *247*, 301−305.
(39) Gonzalez-Pedro, V.; Xu, X. Q.; Mora-Sero, I.; Bisquert, J. Modeling High-Efficiency Quantum Dot Sensitized Solar Cells. *ACS Nano* **2010**, *4*, 5783−5790.
(40) Mora-Sero, I.; Gimenez, S.; Fabregat-Santiago, F.; Gomez, R.; Shen, Q.; Toyoda, T.; Bisquert, J. Recombination in Quantum Dot Sensitized Solar Cells. *Acc. Chem. Res.* **2009**, *42*, 1848−1857.
(41) Bisquert, J.; Fabregat-Santiago, F.; Mora-Sero, I.; Garcia-Belmonte, G.; Gimenez, S. Electron Lifetime in Dye-Sensitized Solar Cells: Theory and Interpretation of Measurements. *J. Phys. Chem. C* **2009**, *113*, 17278−17290.
(42) Gonzalez-Pedro, V.; Sima, C.; Marzari, G.; Boix, P. P.; Gimenez, S.; Shen, Q.; Dittrich, T.; Mora-Sero, I. High Performance PbS Quantum Dot Sensitized Solar Cells Exceeding 4% Efficiency: The Role of Metal Precursors in the Electron Injection and Charge Separation. *Phys. Chem. Chem. Phys.* **2013**, *15*, 13835−13843.
(43) Nelson, J. J.; Amick, T. J.; Elliott, C. M. Mass Transport of Polypyridyl Cobalt Complexes in Dye-Sensitized Solar Cells with Mesoporous TiO_2 Photoanodes. *J. Phys. Chem. C* **2008**, *112*, 18255−18263.
(44) Klahr, B. M.; Hamann, T. W. Performance Enhancement and Limitations of Cobalt Bipyridyl Redox Shuttles in Dye-Sensitized Solar Cells. *J. Phys. Chem. C* **2009**, *113*, 14040−14045.